(with 10000 data points) was generated by the mixing matrix $\mathbf{A} \in \mathbb{R}^{5\times5}$, all the elements of which were drawn from standardised Gaussian distribution (i.e. zero mean and unit variance).

To evaluate the performance of algorithms, we calculated the performance index (*PI*) defined by

$$PI = \frac{1}{n(n-1)}\sum_{i=1}^{n}\left\{\left(\sum_{k=1}^{n}\frac{|g_{ik}|}{\max_j |g_{ij}|}-1\right)+\left(\sum_{k=1}^{n}\frac{|g_{ki}|}{\max_j |g_{ji}|}-1\right)\right\} \quad (10)$$

where g_{ij} is the (i, j)-element of the matrix $\mathbf{G} = \mathbf{WA}$.

We evaluated the performance of three algorithms: JADE [4], SOBI [5], and the proposed algorithm ADDE. All three algorithms are based on the joint approximate diagonalisation but exploit different statistics of the data. For SOBI, 20 different time-delayed correlation matrices of whitened data were exploited. For ADDE, we divided the whitened data into 100 different non-overlapping blocks (the length of each data frame is 100) and calculated 99 differential correlation matrices by considering two adjacent data frames. Although JADE and SOBI are good algorithms, they had difficulty in the presence of nonstationary Gaussian sources with no temporal correlations, as expected. In such a case, the ADDE outperformed JADE and SOBI (see Table 1).

Table 1: Performance of JADE, SOBI and ADDE

Algorithm	Performance index
JADE	0.0146
SOBI	0.0394
ADDE	8.4573×10^{-4}

Discussion: In this Letter, we have introduced the differential correlation and showed that it was useful to capture the time-varying statistics for the case of second-order nonstationary source separation. We have presented an algebraic differential decorrelation method, ADDE, based on the joint approximate diagonalisation. The useful behaviour of the method was confirmed by computer simulations. The ADDE could, in principle, be extended to the case of noisy mixtures. For example, in the presence of temporally white noise, the robust orthogonalisation method (as in [6]) could be applied in our current framework.

Acknowledgment: This work was supported by the Korea Ministry of Science and Technology under the International Co-operative Research Program, the Brain Science Engineering Research Program and by POSTECH BK 21.

13 August 2001
Electronics Letters Online No: 20010932
DOI: 10.1049/el:20010932

Seungjin Choi (*Department of Computer Science and Engineering, Pohang University of Science and Technology, San 31 Hyoja-dong, Nain-gu, Pohang, Kyungbuk 790-784, Korea*)

E-mail: seungjin@postech.ac.kr

A. Cichocki (*Laboratory for Advanced Brain Signal Processing, Brain Science Institute, RIKEN, Japan*)

References

1 CHOI, S., and CICHOCKI, A.: 'Blind separation of nonstationary sources in noisy mixtures', *Electron. Lett.*, 2000, **36**, (9), pp. 848–849

2 CHOI, S.: 'Differential Hebbian-type learning algorithms for decorrelation and independent component analysis', *Electron. Lett.*, 1998, **34**, (9) pp. 900–901

3 DEVILLE, Y., and BENALI, M.: 'Differential source separation: Concept and application to a criterion based on differential normalized kurtosis'. Proc. EUSIPCO, Tampere, Finland, 2000

4 CARDOSO, J.-F., and SOULOUMIAC, A.: 'Blind beamforming for non Gaussian signals', *IEE Proc. F*, 1993, **140**, (6), pp. 362–370

5 BELOUCHRANI, A., ABED-MERAIN, K., CARDOSO, J.-F., and MOULINES, E.: 'A blind source separation technique using second order statistics', *IEEE Trans. Signal Processing*, 1997, **45**, pp. 434–444

6 CHOI, S., CICHOCKI, A., and BELOUCHRANI, A.: 'Blind separation of second-order nonstationary and temporally colored sources'. Proc. IEEE Workshop on Statistical Signal Processing, Singapore, 2001

Correction of frequency-dependent I/Q mismatches in quadrature receivers

K.P. Pun, J.E. Franca, C. Azeredo-Leme, C.F. Chan and C.S. Choy

The I/Q mismatches in wideband receivers designed for multi-channel reception can be frequency-dependent and limit their image rejection performance to an unacceptable level. An adaptive signal-image separation system is proposed to correct the frequency-dependent I/Q mismatches in the digital domain. Simulation results verifying the proposed method are given.

Introduction: In quadrature receivers, it is well known that the amplitude and phase imbalances between the in-phase (I) and quadrature (Q) paths of the demodulator will generate an image component of the received signal. Conventional I/Q mismatch calibration methods [1 - 3] can be used if these errors are frequency-independent. However, when wide receiver bandwidth is of concern, then the frequency dependence of I/Q mismatches must be considered. Among wideband receivers, those designed to accommodate multichannel signals are particularly susceptible to the I/Q mismatches [4], because in such a receiver weak signals and strong signals can be received and digitised together and a strong signal can be the image of a weak one. Therefore, even a small amount of I/Q mismatches can cause the image to overwrite the weak signal. The scenario occurs when the channel selection function of a receiver is brought from the analogue to the digital domain to allow multimode operations [4]. Furthermore, multichannel receivers are very common in base stations.

An adaptive signal separation method was recently proposed for the correction of I/Q mismatches in a complex ΣΔ ADC [5]. In this Letter, a similar system is constructed to correct frequency-dependent I/Q mismatches in quadrature receivers, particularly for multichannel receivers.

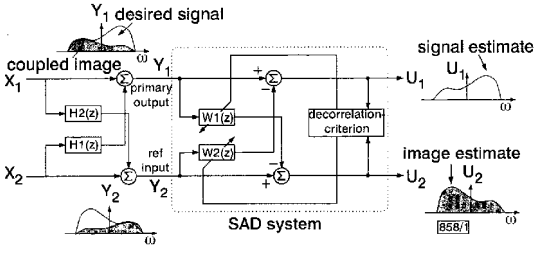

Fig. 1 *SAD signal-image separation system*

I/Q mismatch correction system: Let us denote the ideal (without gain and phase imbalances) I and Q outputs of a receiver as $x_{1,I}(k)$ and $x_{1,Q}(k)$, $k = 0, 1, 2, \ldots$, respectively. Their z-transforms are $X_{1,I}(e^{j\omega})$ and $X_{1,Q}(e^{j\omega})$, respectively. Let us now assume that the I and Q paths have mismatched responses of $H_I(e^{j\omega})$ and $H_Q(e^{j\omega})$, respectively. In the frequency domain, the output of the receiver $Y_1(e^{j\omega})$ can be expressed as

$$\begin{aligned} Y_1(e^{j\omega}) &= H_I(e^{j\omega})X_{1,I}(e^{j\omega}) + jH_Q(e^{j\omega})X_{1,Q}(e^{j\omega}) \\ &= H_{cm}(e^{j\omega})X_1(e^{j\omega}) + H_{dif}(e^{j\omega})X_1^*(e^{-j\omega}) \end{aligned} \quad (1)$$

where $X_1(e^{j\omega}) = X_{1,I}(e^{j\omega}) + jX_{1,Q}(e^{j\omega})$ (the z-transform of $x_1 = x_{1,I} + jx_{1,Q}$), $X_1^*(e^{-j\omega}) = X_{1,I}(e^{j\omega}) - jX_{1,Q}(e^{j\omega})$ (the z-transform of $x_1^* = x_{1,I} - jx_{1,Q}$), and

$$H_{cm}(e^{j\omega}) = [H_I(e^{j\omega}) + H_Q(e^{j\omega})]/2 \quad (2)$$

$$H_{dif}(e^{j\omega}) = [H_I(e^{j\omega}) - H_Q(e^{j\omega})]/2 \quad (3)$$

The mirror image $X_1^*(e^{-j\omega})$ is coupled to the output through the differential term $H_{dif}(e^{j\omega})$ which is generally unknown and possibly time-varying. For perfect channel matching ($H_I(e^{j\omega}) = H_Q(e^{j\omega})$ for all ω), $H_{dif}(e^{j\omega})$ becomes zero and the output will be 'clean', i.e. containing no image components.

If we have a reference signal which is in some way related to the image component, the classical adaptive noise canceller [6] can be used to remove it. A natural source for the reference is the complex conjugate of the received signal, y_1^*. However, this will cause

the well known signal leakage problem [6] as y_1^* contains x_1. To deal with the signal leakage problem, a symmetric adaptive decorrelation (SAD) signal separation algorithm [7] is used here.

Fig. 1 shows the proposed SAD image cancellation system (all the signals and filters in this Figure are complex). In the Figure, x_1 is the desired signal; $x_2 = x_1^*$ is the image; $H_1(z)$ and $H_2(z)$ are the unknown mutual coupling functions ($H_1(z) = H_{dif}(e^{j\omega})$ and $H_2(z) = H_{dif}^*(e^{-j\omega})$); y_1 is the output of the receiver and the primary input to the system; and $y_2 = y_1^*$ is the reference input. The signal estimate $u_1(k)$ and the image estimate $u_2(k)$ are obtained by adaptive filtering of the two inputs:

$$u_i(k) = y_i(k) - \mathbf{w}_i^T(k) \otimes \mathbf{y}_j(k) \qquad i = 1, 2 \quad j = 2, 1 \quad (4)$$

where $\otimes$ represents convolution, $\mathbf{w}_i(k) = [w_i^{(k)}(0)\ w_i^{(k)}(1)\ ...\ w_i^{(k)}(L_i - 1)]^T$ are coefficient vectors of the adaptive filters $W_i(z)$ at time index k, $\mathbf{y}_j(k) = [y_j(k)\ y_j(k-1)\ ...\ y_j(k - L_j + 1)]^T$, and L_i are the filter orders.

The system performs decorrelation between the signal estimate $u_1(k)$ and the image estimate $u_2(k)$. According to this criterion, the filter coefficients are updated as follows:

$$\mathbf{w}_i(k+1) = \mathbf{w}_i(k) + 2\mu_i u_i(k)\mathbf{u}_j^*(k) \qquad i = 1, 2 \quad j = 2, 1 \quad (5)$$

where μ_i are step-sizes which control the speed and stability of the adaptation. μ_i can be chosen as integer powers of 2 for computational efficiency. Since $y_2(k) = y_1^*(k)$, by symmetry we will have $\mathbf{w}_1(k) = \mathbf{w}_2^*(k)$ if $L_1 = L_2$ and $\mu_1 = \mu_2$. If eqn. 5 converges, $u_1(k)$ and $u_2(k)$ will be decorrelated over the span of both filters:

$$C_{u_1u_2}(m) = E[u_1(k)u_2^*(k-m)] = 0 \quad m = 0, ..., L_1 \quad (6)$$

$$C_{u_2u_1}(n) = E[u_2(k)u_1^*(k-n)] = 0 \quad n = 0, ..., L_2 \quad (7)$$

where C means cross-correlation and E represents expected value.

Condition, convergence and noise: A pre-condition of the proposed method is that the desired signal x_1 and its image x_1^* must be uncorrelated with each other. It can be shown that the condition is equivalent to

$$C_{x_{1,I}x_{1,I}}(m) = C_{x_{1,Q}x_{1,Q}}(m) \quad \text{and} \quad C_{x_{1,I}x_{1,Q}}(m) = 0 \qquad m = 0, 1, ..., \max\{L_1, L_2\} \quad (8)$$

Therefore, the desired I and Q signals must have the same self-correlation and must be uncorrelated with each other. In most communication systems, I and Q signals are noise-like and have equal variations. The above conditions are usually satisfied.

Convergence to the desired solution is not guaranteed. However, as suggested in [7], for $|H_1(z)H_2(z)| < 1$ for all z, $z = e^{j\omega}$ and starting from zero initial conditions, the algorithm will most probably converge to the desired solution. In the image cancellation application, $|H_1(z)H_2(z)| = |H_{dif}(e^{j\omega})H_{dif}^*(e^{-j\omega})| \leq |H_{dif}(e^{j\omega})||H_{dif}^*(e^{-j\omega})| \ll 1$, for all ω for most practical situations.

Last, the receiver's output y_1 could also contain additive noise n_a. It is obvious that as long as n_a is not correlated with its image n_a^*, it will not affect the performance of the system.

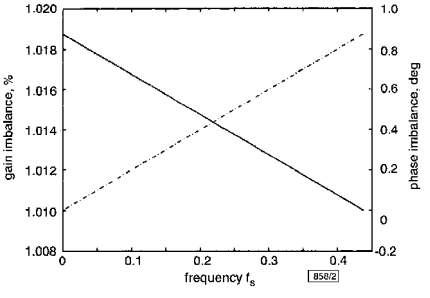

Fig. 2 *Frequency-dependent I/Q mismatch used in simulations*

——— gain mismatch
–·–·– phase mismatch

Real-time computational load: For real-time operation, the required computational power is $(32L)f_s$ floating point operations (FLOPS) per second, where f_s is the output sampling rate of the receiver and L is the system order ($L_1 = L_2 = L$ are assumed). When the system has converged, the updating of filter coefficients can be stopped and the computational load reduces to $(16L)f_s$ FLOPS per second, only a half of the initial requirement.

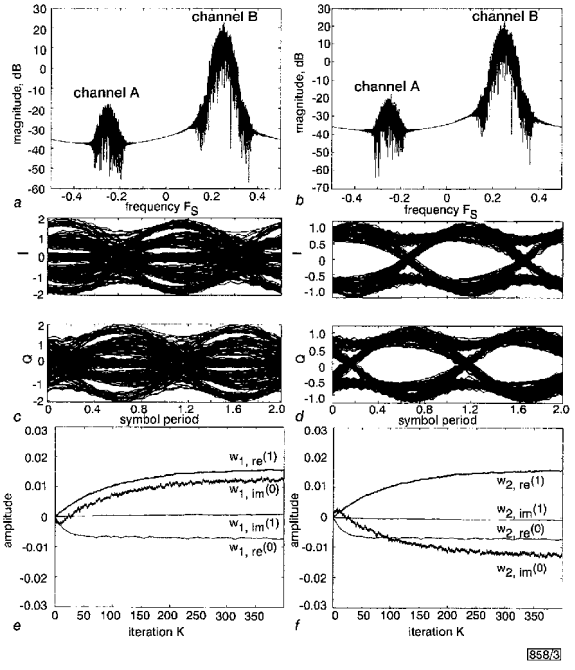

Fig. 3 *Simulation results*

a Input spectrum
b Output spectrum
c Eye-diagram (channel A) before image cancellation
d Eye-diagram (channel A) after image cancellation
e W_1 coefficients of adaptive filter
f W_2 coefficients of adaptive filter

Simulation results: Computer simulations have been conducted with Matlab Simulink™ to verify the proposed frequency-dependent I/Q mismatch cancellation method. In the simulation shown in Fig. 2, the second-order system ($L_1 = L_2 = 2$) is used.

Fig. 3*a* shows the spectrum of the input to the system. It contains two Gaussian-filtered minimum shift keying (GMSK) signals. One is centred at $-f_s/4$ (channel A) and the other at $f_s/4$ (channel B). They are images of each other. Both signals are random GMSK signals with the 3 dB bandwidth-symbol time product of 0.5. Channel B is 40 dB stronger than A. The frequency-dependent I/Q imbalance of the receiver is shown in Fig. 2, which is arbitrarily assigned, but probably worse than most real-world conditions. The mismatch effect is simulated by passing the ideal I and Q signals through two all-pass filters with mismatched gain and phase responses corresponding to Fig. 2. The image components caused by mismatches cannot be observed in Fig. 3*a* owing to the similar shapes of the GMSK signals. However, the effect can be clearly observed from the eye-pattern diagrams of channel A as shown in Fig. 3*c*. The eye-patterns are very noisy and with serious zero-crossing jitters owing to the coupling of channel B to A through I/Q mismatches.

The system output has a spectrum as shown in Fig. 3*b*. Again, the frequency spectrum does not give any information. The eye-pattern diagrams of channel A are shown in Fig. 3*d*. We can find that the eye-patterns become widely opened and only negligible zero-crossing jitter is observed. This means that the image interference owing to frequency-dependent I/Q mismatches has been successfully removed by the signal separation system. The step sizes μ_1 and μ_2 used in this simulation are 2^{-25}. The system converges after 200k iterations as shown in Fig. 3*e* and *f*.

Conclusions: A frequency-dependent I/Q mismatch cancellation method by using the SAD signal separation algorithm has been introduced in this Letter. Computer simulations on a multichannel receiver have demonstrated the effectiveness of the method. The cost is only some additional real-time digital signal processing power.

23 June 2001
Electronics Letters Online No: 20010944
DOI: 10.1049/el:20010944

K.P. Pun, C.F. Chan and C.S. Choy (*The Chinese University of Hong Kong, Shatin, N.T., Hong Kong, People's Republic of China*)

J.E. Franca and C. Azeredo-Leme (*Instituto Superior Técnico, Av. Rovisco Pais 1, 1096 Lisbon, Portugal*)

References

1 CHURCHILL, F.E., OGAR, G.W., and THOMPSON, B.J.: 'The correction of I and Q errors in a coherent processor', *IEEE Trans. Aerosp. Electron. Syst.*, 1981, **AES-17**, (1), pp. 131–137
2 MACLEOD, M.D.: 'Fast calibration of IQ digitiser systems', *Electron. Eng.*, 1990, **62**, (757), pp. 41–43
3 GREEN, R.A., ANDERSON-SPRECHER, R., and PIERRE, J.W.: 'Quadrature receiver mismatch calibration', *IEEE Trans. Signal Process.*, 1999, **47**, (11), pp. 3130–3133
4 VAN DER ZWAN, E., PHILIPS, K., and BASTIAANSEN, C.: 'A 10.7 MHz IF-to-baseband ΔΣ A/D conversion system for AM/FM radio receivers'. Dig. Tech. Papers, IEEE Int. Solid-State Circuit Conf., Feb. 2000, pp. 340–341
5 LI YU, , and SNELGROVE, W.M.: 'A novel adaptive mismatch cancellation system for quadrature IF radio receivers', *IEEE Trans. Circuits Syst., II, Analog Digit. Signal Process.*, 1999, **46**, (6), pp. 789–801
6 WIDROW, B., GLOVER, J.R., Jr., MCCOOL, J.M., KAUNITZ, J., WILLIAMS, C.S., HEARN, R.H., ZEIDLER, J.R., DONG, E., Jr., and GOODLIN, R.C.: 'Adaptive noise cancelling: principles and applications', *Proc. IEEE*, 1975, **63**, (12), pp. 1692–1716
7 GERVEN, S.V., and COMPERNOLLE, D.V.: 'Signal separation by symmetric adaptive decorrelation: stability, convergence, and uniqueness', *IEEE Trans. Signal Process.*, 1995, **43**, (7), pp. 1602–1612

Digital predistortion of wideband signals based on power amplifier model with memory

J. Kim and K. Konstantinou

Memory effects in the power amplifier limit the performance of digital predistortion for wideband signals. Novel algorithms that take into account such effects are proposed. Measured results are presented for single and multicarrier UMTS signals to demonstrate the effectiveness of the new approach.

Introduction: Digital predistortion (DPD) is one of the most promising linearisation techniques that could lead to more efficient and cost effective power amplifiers (PA). The linearisation method intentionally distorts the input signal so that the nonlinearity of the PA can be compensated. In effect, the predistorter has the 'inverse' characteristics of the amplifier to be linearised.

Behaviour models for PA have traditionally been developed based on the AM-AM and AM-PM curves [1, 2], and the PA gain is usually approximated as a complex polynomial function of instantaneous input power level [3, 4]. However, as the bandwidth of the signal increases, memory effects in the transmitter distort this simplified picture. Memory effects are attributed to filter group delays, the frequency response of matching networks, nonlinear capacitances of the transistors and the response of the bias networks. The performance of DPD algorithms that do not take these memory effects into account is severely degraded as the bandwidth of the input signal increases.

In this Letter, a relatively simple model that captures both memory effects and nonlinear behaviour of a PA is proposed. Algorithms that obtain the DPD function based on the estimated model parameters are also described. Measured results are presented for single and multi-carrier universal mobile telecommunication systems (UMTS) input signals to demonstrate the effectiveness of the new approach when compared to memoryless DPD.

Overview of proposed predistortion scheme: The structure of the proposed DPD scheme is shown in Fig. 1. The complex baseband signal u_n and x_n are the input and output of the DPD function, respectively, where n is the time index. x_n is up-converted and fed to the PA. A feedback receiver is used to produce y_n, which is the down-converted and normalised output of the PA. y_n is compared to x_n for characterisation of the PA.

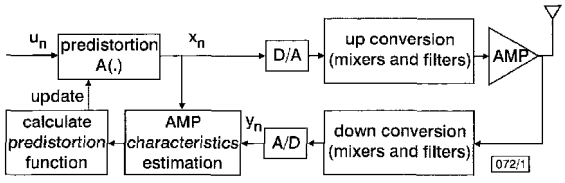

Fig. 1 *Overview of proposed digital predistortion scheme*

The proposed approach is largely divided into two steps. First, the characteristics of PA are estimated, where proper modelling and parameter estimation based on that model are needed. Secondly, the DPD function is obtained by 'inverting' the PA characteristics.

Modelling and estimation of power amplifier: The baseband behaviour of the PA can be described by using a complex polynomial in eqn. 1:

$$\tilde{y}_n \approx x_n \cdot \sum_{k=1}^{k=p} b_k |x_n|^{k-1} \tag{1}$$

where x_n is the complex input of the PA, and $\tilde{y}_n$ is the approximate output of the PA according to the model. p is the order of the polynomial. The above model has the same characteristics over the whole frequency band of operation, which is a good approximation for narrowband signals. However, a real PA has memory and its characteristics depend on the signal frequencies. Having memory means that the output of the PA is not only a function of the current input but also a function of the past inputs and outputs. As the bandwidth of the signal increases, memory effects in the PA become evident. A relatively simple baseband behavioural model that accommodates memory as well as nonlinear behaviour is introduced and described in eqn. 2:

$$\tilde{y}_n = \sum_{m=0}^{m=M} B_m(\mathbf{b}_m, x_{n-m}) \tag{2}$$

where M is the maximum delay in the unit of sample, and

$$\begin{aligned} B_m(\mathbf{b}_m, x_{n-m}) &= x_{n-m} \cdot \sum_{k=1}^{p_m} b_{mk} |x_{n-m}|^{k-1} \\ &= x_{n-m} \cdot \beta_m(|x_{n-m}|) \end{aligned} \tag{3}$$

where p_m is the order of polynomial $B_m(\mathbf{b}_m, x_{n-m})$. The components of vector $\mathbf{b}_m$, $\{b_{m1}, b_{m2}, ..., b_{mp_m}\}$, are complex numbers.

Let $\mathbf{b} \equiv [\mathbf{b}_0 \mathbf{b}_1 ... \mathbf{b}_M]$, then the estimation is obtaining the optimum $\mathbf{b}$ that best describes the characteristics of the PA. We use the minimum mean squared error (MMSE) criterion. Let the error function $f(\mathbf{b})$ be defined as

$$f(\mathbf{b}) \equiv E\left[|y_n - \tilde{y}_n|^2\right] \tag{4}$$

where $E[z]$ is the mean of x. Then, $\mathbf{b}_{opt}$ is the argument of the function f at its minimum. We used the Newton method [5] for the estimation.

Let the estimation error ε be defined as

$$\varepsilon \equiv \min E\left[|\tilde{y}_n - y_n|^2\right] = f(\mathbf{b}_{opt}) \tag{5}$$

The estimation error is an indication of how close the PA model is to the actual PA. Fig. 2 illustrates the effects of adding delay terms in the PA model. The PA tested was an LDMOS, class AB amplifier. A single-carrier UMTS signal and a three-carrier UMTS signal were used as test inputs. Peak limiting was applied so that the peak-to-average power ratio of the signal is 8 dB. The peak output power was near the 1 dB compression point of the PA. We used fifth-order polynomials for all the delay terms, i.e. $p_m = 5$. In the case of narrowband signal, adding more delay terms does not reduce the estimation error much. On the contrary, the estimation error for wideband signals is significantly reduced as the number